Thin-Walled Structures 180 (2022) 109830

Contents lists available at ScienceDirect

Thin-Walled Structures

journal homepage: www.elsevier.com/locate/tws

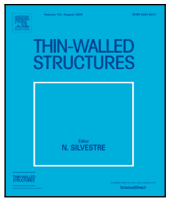

Full length article

Impact resistance of cork-skinned marine PVC / GRP sandwich laminates

L.S. Sutherland *, C. Guedes Sores

Centre for Marine Technology and Ocean Engineering (CENTEC), Instituto Superior Técnico, Universidade de Lisboa, Lisbon, Portugal

ARTICLE INFO

Keywords:
Cork
Impact
Marine
Foam
GRP
Sandwich

ABSTRACT

The introduction of a thin cork layer was investigated as a means to improve the impact resistance of composite foam sandwich laminates whilst maintaining structural performance. Six configurations of this 'cork-skinned' sandwich architecture were evaluated via extensive experimental comparisons with a 'baseline' GRP/ PVC foam sandwich laminate as typically used in marine structures. The concept improved perforation resistance (by up to 60%) for both quasi-static indentation and impact loading rates, albeit with an increase in laminate weight. However, initial (slight) damage resistance and bending strength can be compromised if the detailed laminate architecture is not designed with care.

1. Introduction

Composites, predominantly as glass reinforced plastic (GRP) and/or polymeric foam or balsa-cored sandwich laminates, have now been common in the marine industry for many years, yet their susceptibility to out of plane impact damage is still a concern, especially for sandwich laminates [1–4]. In addition, there is huge momentum for a move towards more sustainable material solutions. Previous investigations [5–12] have shown that the use of cork as a core for composite sandwich construction has the potential to increase absorbed impact energy, and the green credentials of this natural material in terms of sustainability, disposal and recyclability, are well known [13–15]. Despite its very similar ecological credentials and very respectable material properties, especially in compression, end-grain balsa cores are prone to waterlogging, swelling, degradation and rotting when water ingress occurs in the aggressive marine environment. This has been a very common problem for recreational vessels, and has effectively ended the use of this core below the waterline [16–18]. That cork is impervious to water is intuitively known to anyone who enjoys wine, but it also has further advantages in terms of thermal and sound and vibration insulation, fatigue, shape memory retention, and fire retardation properties [12,15,19–24], all of which are important advantages for marine structural materials.

However, despite continuing progress in improving these material properties [23,25–27] cork alternatives still do not match the material properties of the foam cores commonly used in the marine industry [5,6,9,10,12,14,15,28–36]. This is especially true when considering the specific material properties, which are inherently more important in the high-speed craft and super-structure applications where lightweight construction is of prime importance and hence sandwich laminates are of most interest.

Hence, the present study aims to evaluate the engineering effectiveness of a different approach; a laminate architecture design level solution, namely the introduction of a thin cork layer at the impacted surface of the 'traditional' foam sandwich. This approach may be thought of as a functionally graded material (FGM) where the core is 'stepwise graded' (i.e. different cores are bonded together) [37–44]. The use of cork and other natural cores and layers in sandwich laminates has been explored in recent years [45–71]. These studies have considered the effect of different grades of cork [51,55,56,59,60,65,71], thin exterior cork layers as thermal shields [45,46], thin [49,50,53,66] and thicker [53–60,62,65,70,71,71] cork cores. The use of various configurations of a layered sandwich architecture [51,52,63,64,69] and rubber-cork layers under wooden skins, wood layers under GRP skins, and multi-layered wood skinned sandwiches have been found to be beneficial [35,36]. However, to the best knowledge of the authors, the approach proposed here of the simple application of a thin agglomerated cork internal layer onto the core of a traditional GRP/PVC foam marine sandwich laminate in order to improve the impact behaviour, has not yet been investigated.

It is worth noting that to date, studies into the effects of changing the geometric and other parameters of a given type of architecture has been the exception rather than the rule — in almost every case only one specific case of a given concept is studied. This is an extremely important point for contact and impact loading since almost all target/material parameters can significantly influence the behaviour seen [2] and hence considering just one specific permutation of a given laminate architecture may well not lead to the correct, or at least full, conclusions concerning its potential. Unfortunately, it is also usually completely overlooked that better impact response must not come at

* Corresponding author.
E-mail address: l.sutherland@tecnico.ulisboa.pt (L.S. Sutherland).

https://doi.org/10.1016/j.tws.2022.109830
Received 26 October 2021; Received in revised form 30 June 2022; Accepted 17 July 2022
Available online xxxx

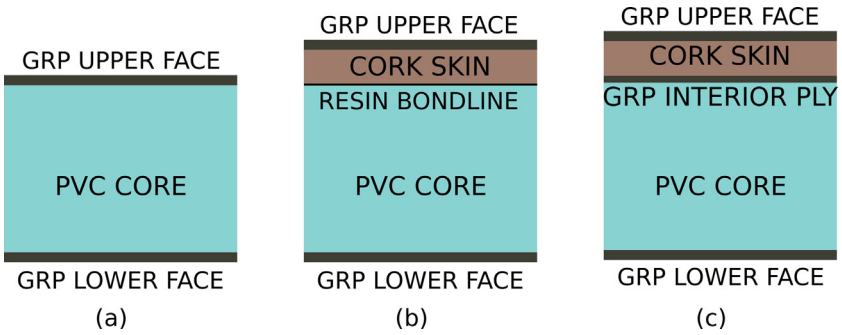

Fig. 1. Sandwich laminate architectures and associated nomenclature.

an unacceptable level of structural performance for many, if not the great majority of, practical application cases.

Hence, to comprehensively evaluate the engineering effectiveness of this concept, various configurations of this sandwich architecture have been compared experimentally with a 'baseline' PVC-GRP (glass reinforced plastic) sandwich as a typical 'traditional' marine laminate. Both quasi-static indentation and impact tests were completed to characterise and compare the indentation and impact behaviour and properties. In addition, long and short beam flexure testing investigated the bending and shear dominated behaviour, respectively, of each cork-skinned laminate to identify any potential significant reductions in engineering properties compared to the 'baseline' PVC sandwich laminate.

2. Sandwich laminate architectures

The 'baseline' sandwich laminate selected was a vacuum assisted hand layup GRP/PVC sandwich laminate of Scott Bader Vinylester VE 679 PA (Pre-accelerated) resin reinforced with 3 plies of 'ETL 800-1270' Biaxial 0/90° 840 g/m^2 E-Glass and a 20 mm thick 'AIREX C70.75.20 P' 80 kg/m^3 cross-linked PVC core (Fig. 1(a)).

The cork-skinned concept is illustrated in its simplest form in Fig. 1(b) (In this paper, this thin cork layer is referred to as a 'skin' to distinguish from the outer GRP 'faces' of the sandwich laminates). The cork was Amorim Cork Composites Lda 'Corecork' NL20 [72] consisting of ground cork granules agglomerated with a proprietary binder. A range of cork-skinned sandwich laminate configurations ('architectures') was considered. To keep the size of the experimental programme to a manageable size, the three parameters thought most likely to influence the impact behaviour were identified as (i) Cork skin thickness, (ii) insertion of an interior GRP ply (between cork skin and PVC core, Fig. 1(c)) and (iii) upper GRP face thickness, with each parameter assigned two possible values

A Corecork layer of less than 2 mm was not thought likely to have any significant effect, and a layer greater than 4 mm would increase both laminate thickness and additional weight of absorbed resin too significantly. The single (to minimise weight gains) 'interior' GRP ply was introduced to form a secondary 'face' sandwich laminate which was thought to possibly improve both impact and mechanical behaviours. A two-ply upper GRP face, together with the single interior ply (where present) gives an alternative equivalence with the three upper face plies of the baseline laminate. The lower GRP face was of three plies in all laminates.

This gave six physically possible candidate cork-skinned laminate architectures plus the 'baseline' simple PVC-cored laminate (Table 1), where the nominal laminate thicknesses shown (assuming a nominal ply thickness of 0.8 mm based on the stipulated nominal fibre volume fraction of 0.4) were validated very well by laminate thickness measurements. One panel of each of these seven sandwich laminates was fabricated by the marine composites specialist Trimarine Compósitos Lda. All reinforcements were hand laminated directly onto the core with warp fibres at 0° using 1.5% catalyst and 99% vacuum. For panels 2 and 3 (c.f. Fig. 1(b)) the Corecork skin was bonded directly to the PVC core with a thin layer of (the thixotropic) resin.

Table 1
Candidate sandwich laminates.

Laminate	Core	Cork skin	Interior ply	Upper plies	Thickness (mm)
1 (baseline)	PVC	None	–	3	24.8
2	PVC	2 mm 'Thin'	–	3	26.8
3	PVC	4 mm 'Thick'	–	3	28.8
4	PVC	2 mm 'Thin'	1	2	26.8
5	PVC	2 mm 'Thin'	1	3	27.6
6	PVC	4 mm 'Thick'	1	2	28.8
7	PVC	4 mm 'Thick'	1	3	29.6

3. Test programme

The test programme consisted of three main parts: (i) Quasi-static (QS) indentation, (ii) Dynamic impact, and (iii) Quasi-static beam flexure (as detailed below in Sections 3.1–3.3, respectively). QS indentation tests serve to characterise and compare laminates for applications where the contact force is applied at very low speeds or statically; for example, walking footfalls on floorings, which involve incident velocities very close to zero [73,74]. Also, the energies to first damage and perforation acquired from these QS indentation tests may be used to estimate the corresponding energies that will be required in impact testing [5,75,76]. Dynamic impact (drop weight) tests serve to characterise and compare laminates for 'low velocity impact' (LVI) events such as tool drops or vessel collisions with floating objects, docks or other craft. Further, any new structural laminate developed for improved impact responses must still perform its primary load-bearing function, and hence long- and short-beam flexural tests validated this for bending and shear dominated behaviours, respectively.

The relevant ASTM standards were used to help design the specific experimental set-ups and specimen sizes to give the required behaviour in each case. To allow valid comparisons to be made, identical experimental set-up and specimen sizes were required for each of the seven different laminates (fabricated panels) considered, and hence the inbuilt 'leeway' integral to these standards was utilised.

3.1. Quasi-static (QS) indentation tests

Since QS and impact test results would be compared, identical test set-ups had to be used in both and hence most of the details of the impact tests are simultaneously being defined in this section. Consideration of the relevant ASTM standards, D7766 [77], D6264 [78] and D7136 [79], resulted in the selection of the rectangular edge-supported geometry of 'Procedure C' (Fig. 2) to avoid damage to the impact machine, and since global plate deflections were expected to be small.

Specimens were simply supported, eliminating any differences in the practically obtainable degree of clamping between static and dynamic tests, and since impact rebounds would not occur due to the planned degree of specimen penetration. A 16 mm Ø hemispherical indenter with a test speed of 0.25 mm/s (to give a test duration of

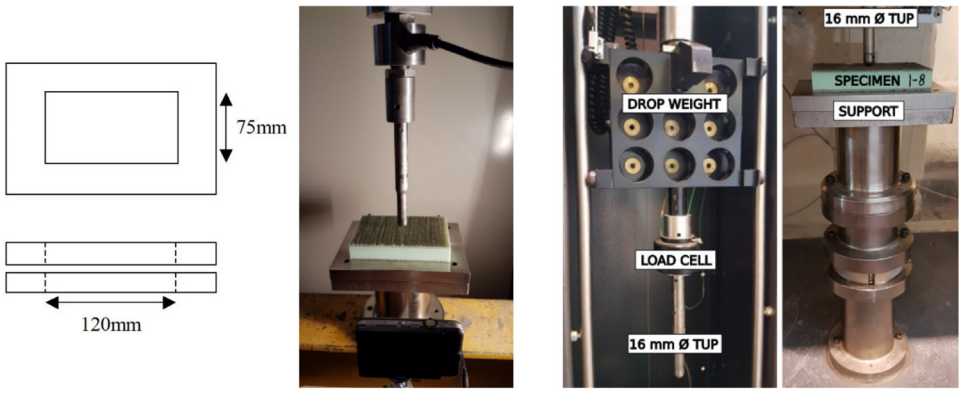

Fig. 2. Test setups: Left to Right, Rectangular support, Quasi-static indentation, and Impact.

approximately 3 min) was used, as suggested in the ASTM standards. A calibrated servo-hydraulic mechanical test machine under constant displacement control was used to quasi-statically indent the surface of the specimen (Fig. 2). Contact force and displacement were recorded and each test stopped at a position 4.5 mm below the height of the top of the support plate to ensure a consistent and full perforation of both top face and core. Video recordings of each test enabled correlation between features of the force–deflection behaviour and observations of physical events and tested specimens were sectioned along the longest centreline with a diamond-surrounded circular saw to enable the damage to be photographed. Three repeat tests for each sandwich laminate were made.

3.2. Impact tests

A Rosand IFW5 instrumented drop weight machine was used for the impact tests (Fig. 2). Specimens were impacted by a variable mass dropped from a measured height and the resulting force recorded by an extremely rigid 'washer' type 60 kN Kistler 9031 A load cell situated between the impact mass and the 'tup' (indenter). A metal flag on the falling weight gave the incident velocity as it passed through an optical gate, thus giving accurate IKE (incident kinetic energy) values and allowing integration of the force versus time data to give displacement and absorbed energy values. Four repeat tests for each sandwich laminate were made. To ensure exact equivalence between impact and QS indentation tests the same physical indenter and support were used for both types of test.

Although Procedure C specifies a fixed mass of 5.5 kg, previous impact testing experience has shown that practically the impact mass may be set to reduce errors due to friction and vibrations without affecting the results [80]. Here, an impact mass of 10.9 kg was found to be optimal and was used for all tests.

The impact incident energies to give equivalent levels of perforation as seen in the QS tests were obtained using a method developed in previous work [5,74,75,81]. The energy absorbed up to the relevant damage events in the QS tests (Section 4.1) were scaled by a 'Dynamic Scaling Factor (DSF)' of 1.6 (empirically derived in previous work on cork cores [5]) to give initial IKE estimates. These values were then refined by preliminary impact tests to give IKE values of 120 J for laminates 1 to 6, and 160 J for laminate 7, which resulted in very similar degrees of perforation as obtained in the equivalent QS tests for each laminate (see Section 4.1). Again, tested specimens were sectioned along the longest centreline with a diamond-surrounded circular saw to enable the damage to be photographed.

3.3. Flexural beam tests

The main aim of the flexural beam tests was to verify that the inclusion of the Corecork skin did not significantly reduce the structural capacity compared to that of the 'baseline' PVC sandwich laminate. Hence, comparisons between the behaviours of the various sandwich laminates were of more interest than the calculation of exact material properties. In order to make valid comparisons, identical test setups had to be used for each sandwich laminate considered, which imposed considerably more constrictions on the details of the test set-up (especially support length) than would normally be encountered when designing these types of tests. The structural performances under both shear and bending dominated conditions were investigated via short- and long-beam flexural tests, respectively.

Table 2
Short-beam flexural test setup.

Loading geometry	3-point
Specimen width, b (mm)	75
Specimen length, L (mm)	450
Support length, S (mm)	300
Support roller diameter (mm)	20
Loading bar 'width' (mm)	50
Test speed (mm/s)	0.5

3.3.1. Short beam flexural tests

The ASTM C393-11 standard, together with preliminary exploratory tests to ensure valid shear failure modes, were used to design short beam flexural tests to check for any possible:

(i) Reduction of shear-controlled beam stiffness due to the Corecork skin
(ii) Premature shear failure in the Corecork skin
(iii) Premature shear failure at the Corecork interfaces
(iv) Premature crushing failure in the Corecork skin

The final short-beam flexure test set-up is given in Table 2. A 3 mm thick rubber pad was placed under the loading roller to offset core crushing [55] and five test repetitions for each laminate were made.

3.3.2. Long beam flexural tests

The ASTM D7249-12 standard, together with preliminary exploratory tests to ensure valid bending failure modes, were used to design long beam flexural tests to check for any possible:

(a) Reduction of bending-controlled beam stiffness due to the Corecork skin
(b) Premature crushing failure in the Corecork skin
(c) Change in axial compressive upper face strength/buckling stability

The standard specimen width of 75 mm and 3-point loading configuration was used, together with a loading bar and 3 mm thick rubber pad under the loading roller to offset core crushing [82].

The final long-beam flexure test set-up is given in Table 3 and five test repetitions for each laminate were made.

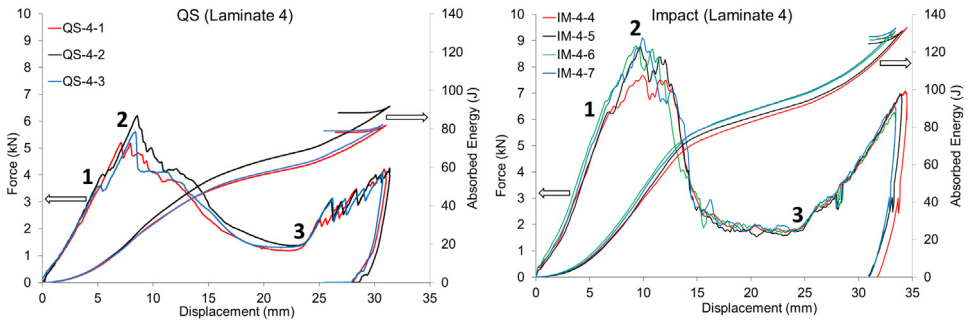

Fig. 3. Typical QS & impact results (Laminate 4).

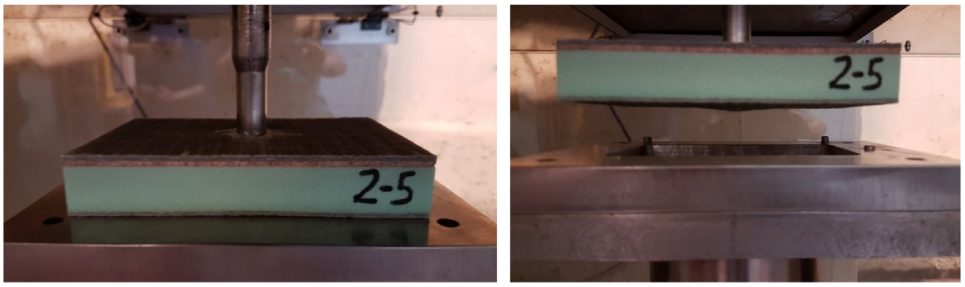

Fig. 4. Full penetration of upper face and contact with lower face.

Table 3
Long-beam flexural test setup.

Loading geometry	3-point
Specimen width, b (mm)	75
Specimen length, L (mm)	900
Support length, S (mm)	850
Support roller diameter (mm)	20
Loading bar 'width' (mm)	50
Test speed (mm/s)	0.3

4. Results

4.1. Impact and QS tests

Tests were very repeatable, in general, and the double-peaked force–displacement and steadily increasing absorbed energy (AE)-displacement behaviours were both very similar in form between QS indentation and impact tests, as illustrated in Fig. 3. However, the laminates were more robust to impact than to QS indentation loading, as further discussed in Section 5.1.

The important features of the force–displacement plots seen for both QS and impact test results (as annotated in the example of Fig. 3) are typical of such tests on laminate sandwich laminates and correspond to the events below [81]:

1. Initial delamination damage (which may occur before or coincident with the maximum force).
2. Maximum force as perforation is initiated with fibre damage and fracture.
3. Complete perforation of the upper face and core as indenter/impactor tup contacts the lower face.

After contact with the lower face, the force again increases and the second peak occurs only because QS tests were consistently stopped at, and impact IKE was set to result in a minimum height of, approximately 4.5 mm below the support height, and as such is not relevant here. An example of full upper face and core perforation is illustrated in Fig. 4.

Hence, the QS and impact behaviour of the various laminates can be compared comprehensively and consistently via the following three responses:

Table 4
Quasi-static indentation results.

Laminate		Initial damage		Maximum load		Perforation	
		Force (kN)	AE (J)	Force (kN)	AE (J)	AE (J)	(Δ%)
1	Average	4.80	18	4.81	20	52	–
	COV	4%	12%	4%	30%	2%	–
2	Average	4.37	14	4.46	15	58	12
	COV	7%	25%	6%	19%	2%	2%
3	Average	4.37	14	4.46	15	58	12
	COV	7%	25%	6%	19%	2%	2%
4	Average	4.27	12	5.67	22	62	19
	COV	20%	37%	9%	20%	7%	7%
5	Average	5.25	18	5.91	29	72	39
	COV	9%	11%	5%	12%	2%	2%
6	Average	3.63	11	4.82	29	58	11
	COV	14%	30%	4%	9%	9%	9%
7	Average	5.37	21	6.84	48	82	58
	COV	7%	17%	4%	6%	4%	4%

(i) Force and absorbed energy at initial damage,
(ii) Maximum Force and absorbed energy to maximum force (penetration),
(iii) Absorbed energy to 'full perforation' of upper face and core.

These responses for each of the seven laminates architectures, with estimates of their variability, are presented in Tables 4 and 5 for QS and impact, respectively, and are discussed in Section 5.1.

The QS and impact perforation failure modes of the sectioned specimens for each of the seven laminate architectures are shown in Figs. 5 and 6, respectively.

4.2. Short-beam flexural tests

All short beam specimens from all laminates exhibited an initial linear force–displacement behaviour, followed by plastic yielding well before final failure. This yielding was not a visible phenomenon but was evident from the force–displacement behaviour (Fig. 7). The Airex PVC manufacturer confirmed that the PVC foam core used here fails in shear plastically, and hence the standard specified 2% shear strain

Fig. 5. Quasi-static failure modes.

Table 5
Impact test results.

Laminate		Initial damage		Maximum load		Perforation	
		Force (kN)	AE (J)	Force (kN)	AE (J)	AE (J)	(Δ%)
1	Average	8.38	34	8.38	34	76	–
	COV	2%	6%	2%	6%	7%	–
2	Average	9.54	42	9.54	42	95	24
	COV	7%	12%	7%	12%	6%	6%
3	Average	9.13	37	9.13	37	94	23
	COV	5%	19%	5%	19%	7%	7%
4	Average	6.55	21	8.59	42	90	18
	COV	3%	6%	7%	4%	3%	3%
5	Average	7.39	24	10.12	58	113	48
	COV	2%	13%	5%	16%	4%	4%
6	Average	5.95	19	8.54	58	94	24
	COV	6%	13%	3%	8%	1%	1%
7	Average	7.89	28	9.80	82	122	59
	COV	9%	21%	6%	10%	6%	6%

offset method was used to give the failure load. Final collapse (due to core crushing, upper face failure, or Corecork shear failure) then occurred well after plastic shear failure (in terms of displacement) and gave very little reserve load-bearing capacity.

The initial stiffness, k_i, and maximum force, P_{max} results from the force–displacement behaviour plots provide intuitive and consistent engineering interpretations of the data capable of identifying any reductions in shear-controlled beam stiffness or beam shear load-bearing capacity due to the Corecork skin.

Further, to try to take into account the effects of the differences in sandwich thickness between the various laminates, and to give an estimate of the laminates' material properties, the panel shear rigidity, U (kN), was calculated using Eq. (1) [83]:

$$U = \frac{S}{4\left(1/k_i - S^3/48D\right)} \tag{1}$$

where, S = support length (mm), k_i = initial stiffness (kN/mm) and D (kN mm ^{2}) is given by:

$$D = \frac{E_1 t_1 E_2 t_2 (d+c)^2 b}{4\left(E_1 t_1 + E_2 t_2\right)} \tag{2}$$

Fig. 6. Impact failure modes.

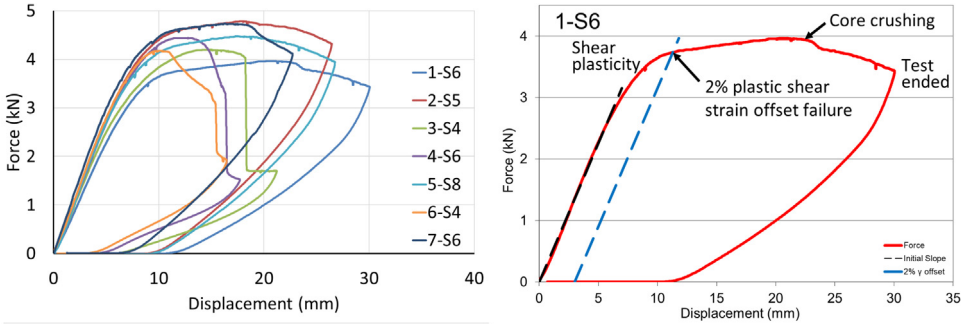

Fig. 7. Representative examples of short-beam behaviour.

where, E = facing modulus (MPa), t = facing thickness (mm), d = sandwich thickness (mm), c = core thickness (mm), b = sandwich width (mm), and subscripts *1* and *2* are for upper (compressive) and lower (tensile) faces, respectively.

Table 6
Short-beam flexural test results.

Laminate	1		2		3		4	
	Average	COV	Average	COV	Average	COV	Average	COV
Initial Stiffness, k_i (kN/mm)	0.45	1.0%	0.54	2.1%	0.48	3.7%	0.53	1.8%
Panel Shear Rigidity, U (kN)	43.56	1.3%	52.10	2.8%	43.57	4.3%	51.29	1.9%
Maximum Load, P_{max} (kN)	3.99	2.0%	4.71	2.2%	4.20	3.8%	4.43	1.9%
Shear Ult. Strength, F_s^{yield} (MPa)	1.10	2.1%	1.20	2.8%	1.01	3.3%	1.21	1.3%
Laminate	5		6		7			
	Average	COV	Average	COV	Average	COV		
Initial Stiffness, k_i (kN/mm)	0.52	2.4%	0.53	1.0%	0.56	1.2%		
Panel Shear Rigidity, U (kN)	49.57	3.1%	48.86	1.2%	50.50	1.3%		
Maximum Load, P_{max} (kN)	4.51	2.2%	4.17	1.5%	4.74	1.3%		
Shear Ult. Strength, F_s^{yield} (MPa)	1.12	2.1%	1.04	1.3%	1.13	0.8%		

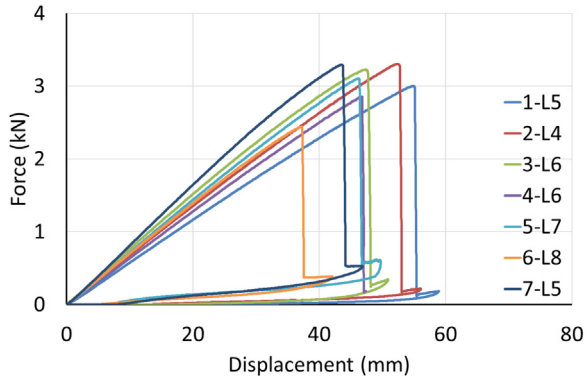

Fig. 8. Representative examples of long-beam behaviour.

Facing moduli values of E_1 = 23 400 MPa and E_2 = 26 390 MPa obtained for a nominally identical GRP laminate as part of the MOSAIC project [84] were used. A nominal ply thickness [82] of 0.8 mm (derived from the fibre areal weight and the fibre volume fraction) together with the total number of plies in the upper face, including any interior ply, were used to calculate the relevant facing thicknesses.

Finally, the shear yield strengths were calculated using Eq. (3) [82].

$$F_s^{yield} = \frac{P_{yield}}{(d+c)\,b} \tag{3}$$

where, F_s^{yield} = core shear ultimate strength (MPa), P_{yield} = force at 2% offset shear strain (N).

The shear-dominated short beam flexural results are given in Table 6 for each sandwich laminate architecture and are further discussed in Section 5.2.1.

4.3. Long-beam flexural tests

All long beam specimens from all laminates exhibited an initial linear force–displacement behaviour, followed by sudden failure (Fig. 8). The videos of each test confirmed this to be due to wrinkling/buckling failure of the upper face, as shown in Fig. 9.

Again, the initial stiffness, k_i, and maximum force, P_{max} results from the force–displacement behaviour plots provide intuitive and consistent engineering interpretations of the data capable of identifying any reductions in bending-controlled beam stiffness or beam bending load-bearing capacity due to the Corecork skin.

Further, to try to take into account the effects of the differences in sandwich thickness between the various laminates, and to give an estimate of the material properties, the panel bending stiffness, D (kN mm^2), was calculated by rearranging Eq. (1):

$$D = \frac{S^3}{48\,(1/k_i - S/4U)} \tag{4}$$

where, the relevant values of U (kN) in Table 6 from the short-beam tests were used.

Finally, the upper facing compressive strengths were calculated from the maximum (failure) loads using Eq. (5) [85].

$$F^{ult} = \frac{P_{max} \cdot S}{2\,(d+c)\,bt} \tag{5}$$

where, F^{ult} = upper facing compressive ultimate stress (MPa), P_{max} = maximum force prior to failure, (N), t = nominal upper facing thickness (mm), d = measured sandwich total thickness (mm), c = calculated core thickness (mm), b = specimen width (mm), and S = support span length (mm).

Frame by frame video analysis showed that for all tests where an interior ply was present (laminates 4 to 7) compression failure occurred simultaneously throughout the upper face GRP-Corecork 'face sandwich', and not solely in the face or interior GRP plies (Fig. 9). Hence, in these cases, the calculated values of facing ultimate stress were based on the total number of upper GRP plies (i.e. upper face plus interior plies). Again, as per the relevant standard [85] the same nominal ply thickness of 0.8 mm was used to calculate the face laminate thickness.

The bending-dominated long beam flexural results are given in Table 7 for each sandwich laminate architecture and are further discussed in Section 5.2.2.

5. Discussion

The results given in Section 4 are now discussed and interpreted in terms of the engineering effects of substituting the 'baseline' simple PVC sandwich laminate with the various candidate configurations of the 'Corecork-skinned' sandwich laminate concept. The behaviour seen is evaluated for each of the various properties investigated, i.e. QS indentation, impact, and shear- and bending-dominated flexure. Further, these properties are quantified in terms of each of the various measured responses. For reference, Table 1 gives the lay-ups of the baseline and six 'Corecork-skinned' sandwich laminates.

5.1. Quasi-static indentation and impact

The behaviour seen in Fig. 3 is typical of the out of plane contact indentation/impact of a GRP laminate, with points '1' and '2' corresponding to initial delamination, and fibre damage at the start of the penetration process that leads to complete perforation, respectively [2].

5.1.1. Initial damage

An increase in the force or energy to first damage indicates a higher resistance to initial damage. Generally, very similar trends with change in sandwich laminate architecture were seen between the force and absorbed energy to initial damage, but these trends were not the same for QS indentation and impact loading rates (Fig. 10).

Fig. 10 shows that only those laminates with four GRP plies in the upper Corecork skin face (laminates 5 and 7) show any improvement in

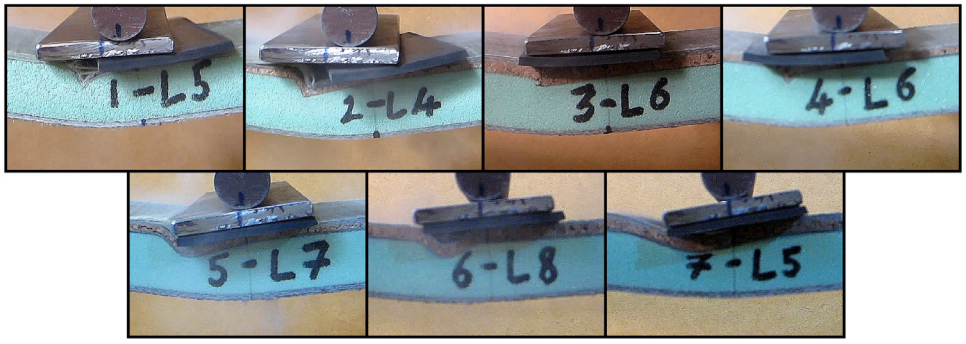

Fig. 9. Long-beam upper face failures.

Table 7
Long-beam flexural test results.

Laminate	1		2		3		4	
	Average	COV	Average	COV	Average	COV	Average	COV
Initial Stiffness, k_i (kN/mm)	0.06	0.5%	0.07	0.8%	0.07	2.3%	0.06	0.5%
Panel Bending Stiffness, D (kN-mm^2)	1.06E6	0.7%	1.19E6	1.2%	1.45E6	3.6%	1.12E6	0.7%
Failure Load, P_{max} (kN)	3.14	4.9%	3.29	3.1%	3.10	5.1%	2.85	1.4%
Facing Ultimate Stress, F^{ult} (MPa)	162.69	4.8%	157.99	2.6%	136.71	4.8%	135.01	1.3%
Laminate	5		6		7			
	Average	COV	Average	COV	Average	COV		
Initial Stiffness, k_i (kN/mm)	0.07	0.6%	0.07	1.0%	0.08	1.0%		
Panel Bending Stiffness, D (kN-mm^2)	1.34E6	0.8%	1.26E6	1.5%	1.61E6	1.5%		
Failure Load, P_{max} (kN)	3.09	2.6%	2.47	4.6%	3.25	3.0%		
Facing Ultimate Stress, F^{ult} (MPa)	107.68	2.8%	107.31	4.5%	104.75	2.6%		

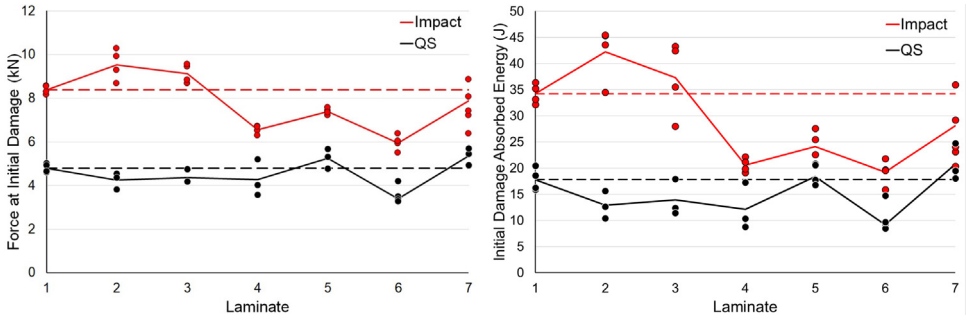

Fig. 10. Initial damage force and energy.

resistance to initial damage due to QS indentation loading over that of the baseline simple PVC sandwich laminate. Further, even if this effect is real and not just due to experimental scatter (especially for laminate 5) it is not a large improvement. All other Corecork skin laminates considered here (laminates 2, 3, 4 and 6) have a reduced resistance to initial damage due to QS indentation loading (compared to that of the baseline laminate 1).

However, for the case of dynamic impact loading, Fig. 10 shows that only those laminates with a Corecork skin without an interior GRP ply (laminates 2 and 3) show any improvement in initial damage resistance over that of the baseline laminate 1. All of the other Corecork skin laminates considered here (laminates 4, 5, 6 and 7) offer less resistance to initial damage due to impact loading than does the baseline laminate.

5.1.2. Maximum force

In general, the maximum force and the energy absorbed up to this maximum force are concurrent with the initiation of severe damage and the start of perforation, as 'penetration' begins. Fig. 11 shows that the variation of maximum force and its associated absorbed energy with laminate architecture is similar but not identical for QS and impact loading rates. In general, the absorbed energy to the onset of severe damage increases with Corecork skin thickness and the number of GRP interior and upper face plies.

For QS indentation loading, Fig. 11 indicates that those laminates with no interior GRP ply and thin and thick Corecork skins (laminates 2 and 3, respectively) perhaps show a very slight reduction in resistance to the onset of severe damage/penetration. However, all of the Corecork-skinned laminate architectures with an interior GRP ply (laminates 4, 5, 6 and 7) show some degree of increased resistance to severe damage/penetration, with this effect strongest for a thick Corecork skin, and one and three interior and upper face GRP plies, respectively (laminate 7).

Further, considering dynamic impact loading, Fig. 11 indicates that all Corecork-skinned laminates are, to various degrees, better at resisting the onset of severe damage/penetration than the baseline laminate, especially when considering the energy required. Again, those laminates with an interior GRP ply perform better in this respect, with a thick Corecork skin, and one and three interior and upper face GRP plies, respectively, (laminate 7) providing the highest resistance.

5.1.3. Perforation energy

Perforation of the laminate is an important impact resistance criterion in a marine setting. Here it has been defined as the full perforation

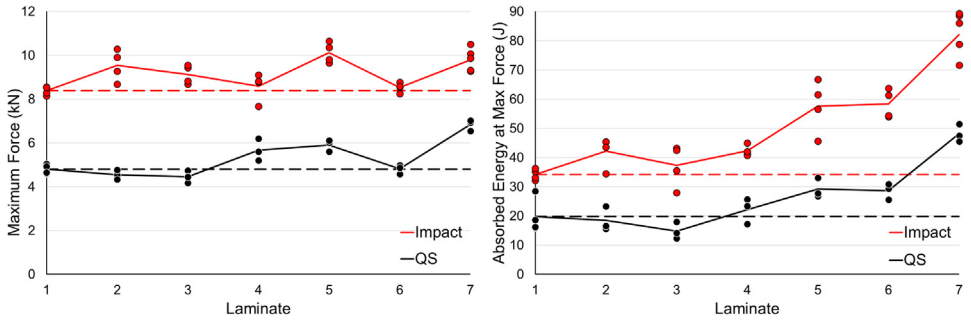

Fig. 11. Maximum force and absorbed energy to maximum force.

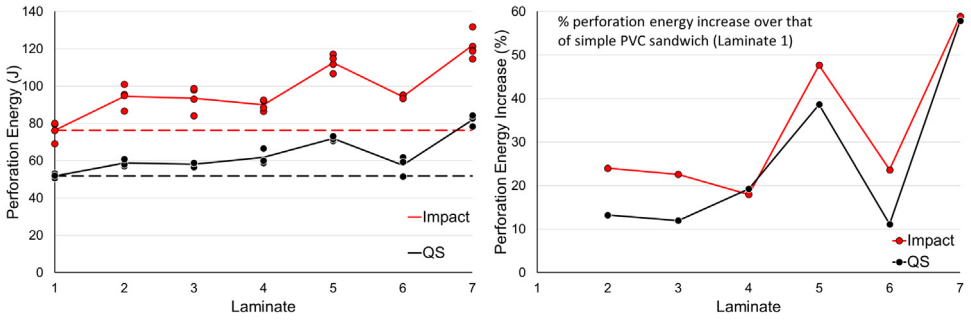

Fig. 12. Perforation energy.

of the upper, contacted skin and the (much less resistant) core as an objective, repeatable measure. Fig. 12 clearly shows that resistance to perforation is higher for both QS indentation and impact loading rates for all Corecork-skinned laminates compared to the baseline laminate.

Further, Fig. 12 also shows that when these increases in perforation energy are expressed as percentage increases over that of the baseline laminate, up to a 60% improvement is seen. The trends in perforation energy with Corecork-skinned laminate architecture are broadly similar for both QS indentation and impact loading rates, with slightly better perforation resistance improvements for impact than for QS loading for most of the sandwich laminate architectures considered here.

The best resistance to perforation is shown by laminates 5 and 7 with approximately 40 and 60% improvements in perforation energy over that of the baseline laminate, respectively. Both of these laminates have four GRP plies in the upper face compared to the baseline's three, and hence the increase in perforation resistance may be in part due to this. However, the fact that the thicker Corecork skin of laminate 7 gives an extra increase of approximately 20% in perforation energy over the thinner Corecork skin of laminate 5 indicates that the inclusion of the Corecork is also important (since both laminates have a total of 4 upper face GRP plies). For all other Corecork-skinned laminates (laminates 2, 3, 4 and 6), the increase in perforation energy is between approximately 10 and 20% for QS indentation, and 20 and 25% for impact.

However, all of the Corecork-skinned laminates are heavier than the baseline simple PVC core, and laminates 5 and 7 further add to this with the weight of an extra GRP ply. Hence, to try to express the 'weight efficiency' of these increases in perforation energy, Fig. 13 compares the ratio of increase in perforation energy to the ratio of increase in measured laminate areal density (Table 8), both with respect to the baseline laminate 1. This plot indicates that the laminate with two upper face GRP plies, a thin Corecork skin and one interior GRP ply (laminate 4) provides the most 'weight efficient' solution for improved perforation resistance.

Table 8
Laminate areal densities.

Laminate	Areal density	
	(kg/m^2)	(Δ%)
1	9.26	–
2	10.35	11.8
3	10.80	16.6
4	9.93	7.1
5	11.32	22.2
6	10.92	17.9
7	12.05	30.1

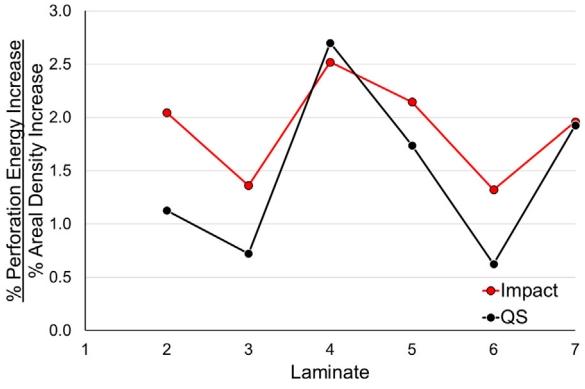

Fig. 13. Weight adjusted increase in perforation resistance (w.r.t. baseline laminate).

5.1.4. Failure modes

Below, initial hypotheses linking the behaviour seen to the perforation damage are suggested. However, it is important to note that further investigations, specifically designed to explore the different stages of damage incurred and guided by the results of this investigation would be required to corroborate, or otherwise, these hypotheses. It should also be remembered that, depending on the exact application, an increase in damage can be advantageous (due to increased energy absorption) or disadvantageous (due to associated reductions to laminate performance).

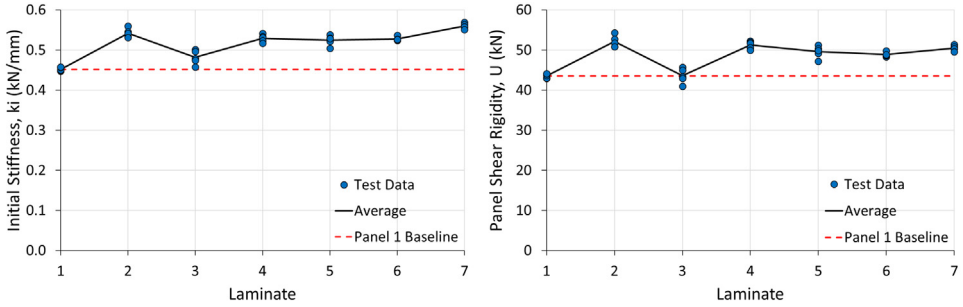

Fig. 14. Short-beam initial stiffness and shear rigidity.

Core Damage: Since all of the QS and Impact tests in this study were designed to give a consistent level of damage, i.e. until full penetration of the core, the damage to the core seen was generally very similar in all cases, with crushing and splitting giving a cavity that was occupied by the indentor/impactor, together with shear cracks emanating around the bottom of this cavity to the bottom face. However, some slight differences were seen as described below.

Differences between QS and Impact Damage: In general, there is significantly more delamination of the upper laminate(s) for impact than for QS loading. This is especially true for the 'baseline' GRP/PVC sandwich laminate 1, and for laminates 2 and 3 with Corecork layers but no interior GRP ply, which could explain the large differences between Impact and QS absorbed energies seen for these three laminates in Fig. 10. This may well help to explain why the 'Dynamic Scaling Factor (DSF)' used in Section 3.2 and seen in previous work [5,81] is greater than 1.

For sandwich architectures with an interior GRP ply (laminates 4 to 7) impact tests also give more delamination than the QS tests, but this is mainly between the interior ply and the Corecork skin, and for laminates 6 and 7 with thicker Corecork skins this difference is marginal since these two architectures already suffer a higher degree of Corecork-interior GRP ply delamination under QS loading than do the other architectures studied here. These damage trends correspond to the relatively smaller differences between QS and impact AE shown in Fig. 10 for laminates 4 to 7, and perhaps indicates that delamination damage to the upper face absorbs the majority of the impact energy, whilst that of an interior ply is not so important in this respect.

Effect on damage of the inclusion of a Corecork skin (laminates 2 and 3): For QS testing this appears to have very little effect at all on the visible impact damage, but the slight decrease in AE with the introduction of a Corecork skin seen in Fig. 10 indicates that perhaps the Corecork reduces the damage to the upper face laminate. For impact testing the Corecork significantly reduces the upper face delamination and core crushing outside of the contact area, but the slight increase in AE with the introduction of a Corecork skin seen in Fig. 10 indicates that perhaps other failure mechanisms are more important in terms of absorbed energy.

Effect on damage of the inclusion of an interior GRP ply (laminates 4 to 7): For QS and impact loading, this appears to introduce delamination at the Corecork – interior GRP ply interface whereas there was no visible delamination of the simple Corecork – PVC foam resin bonded interface in laminates 2 and 3. However, Fig. 10 shows both no significant trend of increased QS AE and a marked reduction in absorbed energy for impact loading with the inclusion of an interior GRP ply. This perhaps indicates that this damage absorption mechanism is not significant for QS and impact loading, and/or that it may reduce the severity of other impact damage mechanism(s) which contribute more significantly to energy absorption.

5.2. Structural performance

Shear-dominated flexural failure was due to plastic shear yielding of the PVC foam core. Bending-dominated flexural failure was due to compressive/buckling failures of the upper 'face' (which here includes the Corecork skin and interior GRP ply, where applicable). Fig. 9 shows that the exact nature of this upper face failure mode did vary. The inclusions of an interior GRP ply and a thicker Corecork skin appear to have reduced the amount of compression damage to the GRP upper plies (as seen in laminates 1 and 2) and favoured a more global upper GRP/Corecork 'face sandwich' pure buckling mode (as seen for laminates 5, 6 and 7). Failure of the upper GRP/Corecork 'face sandwich' appears to have been initiated in the 'interior' GRP ply for laminates 3 and 4. However, deeper investigation into the exact natures of the complex, multifarious and interacting micromechanical failure modes responsible for these effects is not within the scope of this work. The engineering repercussions, in terms of flexural properties, of the various Corecork skin architectures studied here are discussed below.

5.2.1. Shear-dominated flexural behaviour

The short-beam results of Section 4.2 are discussed below in terms of the possible reductions in the shear-dominated structural performance effects due to the inclusion of a cork skin (see Section 3.3.1).

(i) Shear-controlled beam stiffness: Fig. 14 shows that none of the candidate Corecork-skinned laminates suffered a reduction in shear rigidity compared to the baseline laminate. In fact, all except laminate 2 are at least 10% stiffer than the baseline in terms of shear.

(ii) and (iii) Premature shear failure: Fig. 15 shows that the shear load capacities of all of the candidate Corecork-skinned sandwiches are greater than that of the baseline laminate. When shear stress is calculated, the values for laminates 2, 4, 5 and 7 are greater than or equal to that of the baseline laminate, whereas laminates 3 and 6 give slightly lower values.

Further, all calculated shear strengths were higher than the manufacturer's values for Airex C70-75 PVC [86] and NL20 Corecork [72] (Fig. 15). Hence, all the evidence indicates that there was no premature shear failure in the Corecork skin and/or at the Corecork interfaces.

(iv) Premature core crushing: Fig. 16 shows that the Corecork-skinned laminates sustained at least as much compression as the baseline laminate. Further, these values all lie within the bounds of the Airex C70.75 PVC foam manufacturer's quoted minimum and average compressive strengths [86], and close inspection of the test videos showed that core crushing initiated in the PVC core, and not in the Corecork skin, in all cases. Hence, there is no evidence that there was premature crushing failure in the Corecork skin, or indeed premature PVC core crushing in the Corecork-skinned laminates.

5.2.2. Bending-dominated flexural behaviour

The long-beam results of Section 4.3 are discussed below in terms of the possible reductions in the bending-dominated structural performance effects due to the inclusion of a cork skin (see Section 3.3.2).

(a) Bending-controlled beam stiffness: The plots of long-beam (bending-controlled) initial force–displacement stiffness and calculated panel bending stiffness, D, in Fig. 17 show that none of the candidate Corecork-skinned laminates suffered a reduction in bending stiffness

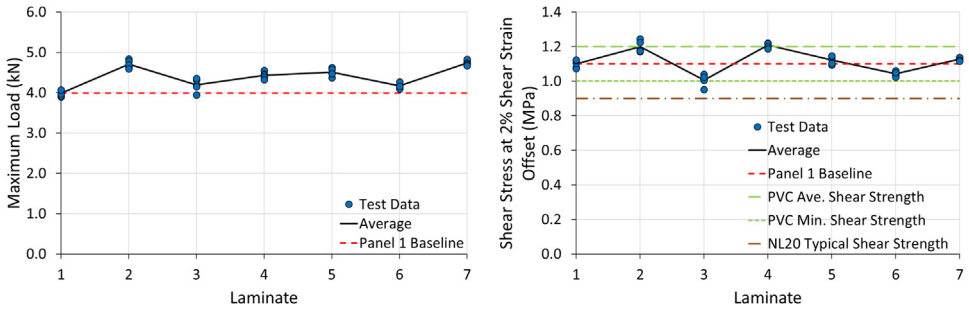

Fig. 15. Short beam failure load and shear strength (2% shear strain offset).

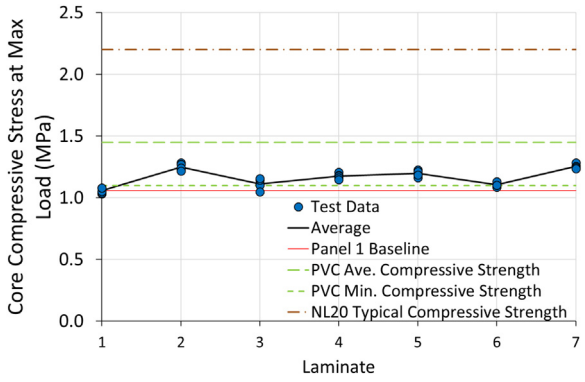

Fig. 16. Short-beam core compressive stress at maximum load.

compared to the baseline laminate. In fact, all Corecork laminates were stiffer than the baseline laminate in terms of bending.

(b) Premature crushing failure in the Corecork skin: Fig. 18 shows that the loading bar induced core compressive stress at long-beam failure is close to that of the baseline laminate except for laminate 6.

However, all of the core compressive stress values at beam failure are significantly lower than both the Airex C70.75 PVC foam [86] and Corecork [72] manufacturer's quoted compressive strengths, indicating that core crushing was not significant in long-beam failure modes. Further, close inspection of the test videos confirmed both that any core crushing observed occurred in the PVC core and not in the Corecork skin in all cases, and importantly, was initiated by the preceding wrinkling/buckling failure of the upper face laminate(s). Hence, all the evidence indicates that there was no premature crushing failure in the Corecork skin, or indeed premature PVC core crushing in the Corecork-skinned laminates.

(c) Compressive skin strength/buckling stability: Fig. 18 shows that the bending load capacities of the Corecork-skinned laminates with three upper GRP plies (laminates 2, 3, 5 and 7) are not significantly lower than that of the baseline laminate. However, those Corecork-skinned laminates with only two upper GRP plies do have a reduced bending load bearing capacity (laminates 4 and 6), especially the thick Corecork-skinned laminate 6. This is almost certainly due to the decreased buckling stability of these thinner upper laminates, where bending induced compressive forces are highest.

6. Conclusions

The introduction of a thin cork (Corecork NL20) layer has been investigated as a means to increase impact energy absorption in composite sandwich construction. Six different sandwich architecture configurations were studied via extensive quasi-static indentation and drop-weight impact experimental comparisons with a 'baseline' GRP/PVC foam sandwich laminate as typically used in marine structures. To verify that any improvements in indentation and/or impact performance were not at the cost of reduced structural properties, long and short beam flexure tests investigated the different laminates' bending and shear dominated behaviours, respectively.

The performance and ranking of the laminate architectures varied with both damage resistance criteria (initial, penetration and perforation damage) and loading (quasi-static indentation, impact, shear and bending). Hence, any discussion of 'good' or 'improved' impact behaviour must also indicate the impact failure criteria and loading rate as well as any possible effects on structural load bearing performance.

Overall, the concept was found to improve the perforation resistance (by up to 60%) for both quasi-static indentation and impact loading rates, albeit with an increase in laminate weight. However, initial (slight) contact damage resistance and beam bending strength can be compromised if the laminate architecture is not designed with care. Beam shear- and bending-dominated stiffness, and shear-dominated load-bearing capacity was not compromised, but laminates with one less GRP ply in the upper, contacted face were slightly weaker in bending dominated beam loadings. Better resistance to all levels of damage for dynamic impact loading rates than for QS indentation was evident, and failure modes differed slightly between QS and impact, indicating that damage mechanisms are loading rate dependent.

CRediT authorship contribution statement

L.S. Sutherland: Writing – review & editing, Writing – original draft, Visualization, Methodology, Investigation, Funding acquisition, Formal analysis, Data curation, Conceptualization. **C. Guedes Sores:** Writing – review & editing, Project administration.

Declaration of competing interest

The authors declare that they have no known competing financial interests or personal relationships that could have appeared to influence the work reported in this paper.

Funding

This work was supported by Amorim Cork Composites S.A., Portugal (Project No. ADIST 1802P.00266). Dr. Sutherland was funded by the FCT (Fundação para a Ciência e Tecnologia), contract No. IST-ID/164/2018. This work contributes to the Strategic Research Plan of the Centre for Marine Technology and Ocean Engineering (CENTEC), which is financed by the Portuguese Foundation for Science and Technology (Fundação para a Ciência e Tecnologia - FCT) under contract UIDB/UIDP/00134/2020.

Data availability

The authors do not have permission to share data.

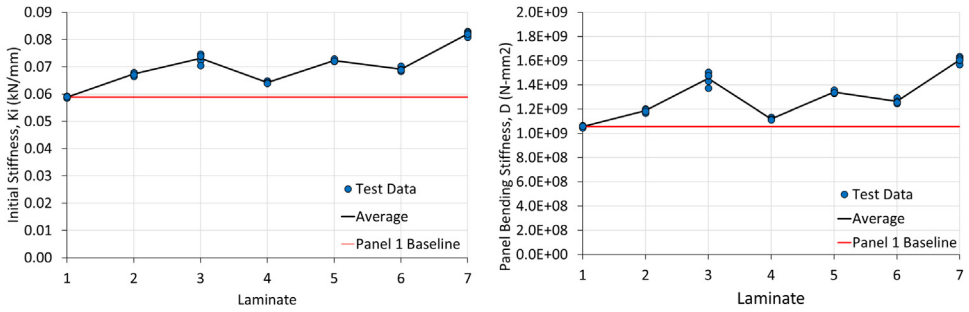

Fig. 17. Long-beam initial stiffness and bending stiffness.

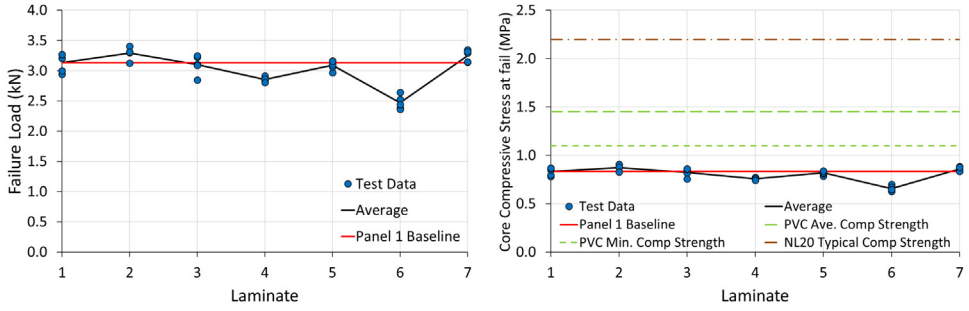

Fig. 18. Long-beam core compressive stress and load at failure.

References

[1] L.S. Sutherland, A review of impact testing on marine composite materials: Part I – Marine impacts on marine composites, Compos. Struct. 188 (2018) 197–208, http://dx.doi.org/10.1016/j.compstruct.2017.12.073.

[2] L.S. Sutherland, A review of impact testing on marine composite materials: Part II – Impact event and material parameters, Compos. Struct. 188 (2018) 503–511, http://dx.doi.org/10.1016/j.compstruct.2018.01.041.

[3] L.S. Sutherland, A review of impact testing on marine composite materials: Part III - Damage tolerance and durability, Compos. Struct. 188 (2018) 512–518, http://dx.doi.org/10.1016/j.compstruct.2018.01.042.

[4] L.S. Sutherland, A review of impact testing on marine composite materials: Part IV - scaling, strain rate and marine-type laminates, Compos. Struct. 200 (2018) 929–938, http://dx.doi.org/10.1016/j.compstruct.2018.06.052.

[5] T. Castilho, L.S. Sutherland, C. Guedes Soares, Impact resistance of marine sandwich composites, in: Marit. Technol. Eng. - Proc. MARTECH 2014 2nd Int. Conf. Marit. Technol. Eng., Taylor & Francis Group, London, UK, 2015, pp. 607–618.

[6] S. Petit, C. Bouvet, A. Bergerot, J.-J. Barrau, Impact and compression after impact experimental study of a composite laminate with a cork thermal shield, Compos. Sci. Technol. 67 (2007) 3286–3299, http://dx.doi.org/10.1016/j.compscitech.2007.03.032.

[7] S. Sanchez-Saez, E. Barbero, J. Cirne, Experimental study of agglomerated-cork-cored structures subjected to ballistic impacts, Mater. Lett. 65 (2011) 2152–2154, http://dx.doi.org/10.1016/j.matlet.2011.04.083.

[8] I. Alcântara, F. Teixeira-Dias, M. Paulino, Cork composites for the absorption of impact energy, Compos. Struct. 95 (2013) 16–27, http://dx.doi.org/10.1016/j.compstruct.2012.07.015.

[9] C. Sergi, S. Boria, F. Sarasini, P. Russo, L. Vitiello, E. Barbero, S. Sanchez-Saez, J. Tirillò, Experimental and finite element analysis of the impact response of agglomerated cork and its intraply hybrid flax/basalt sandwich structures, Compos. Struct. 272 (2021) 114210, http://dx.doi.org/10.1016/j.compstruct.2021.114210.

[10] I. Ivañez, S. Sánchez-Saez, S.K. Garcia-Castillo, E. Barbero, A. Amaro, P.N.B. Reis, High-velocity impact behaviour of damaged sandwich plates with agglomerated cork core, Compos. Struct. 248 (2020) 112520, http://dx.doi.org/10.1016/j.compstruct.2020.112520.

[11] F. Sarasini, J. Tirillò, L. Lampani, E. Barbero, S. Sanchez-Saez, T. Valente, P. Gaudenzi, C. Scarponi, Impact behavior of sandwich structures made of flax/epoxy face sheets and agglomerated cork, J. Nat. Fibers 17 (2020) 168–188, http://dx.doi.org/10.1080/15440478.2018.1477084.

[12] C. Sergi, J. Tirillò, F. Sarasini, E. Barbero Pozuelo, S. Sanchez Saez, C. Burgstaller, The potential of agglomerated cork for sandwich structures: A systematic investigation of physical, thermal, and mechanical properties, Polymers 11 (2019) 2118, http://dx.doi.org/10.3390/polym11122118.

[13] H. Pereira, Cork: Biology, Production and Uses, first ed., Elsevier, Amsterdam, London, 2007.

[14] J. Sargianis, H. Kim, J. Suhr, Natural cork agglomerate employed as an environmentally friendly solution for quiet sandwich composites, Sci. Rep. 2 (2012) http://dx.doi.org/10.1038/srep00403.

[15] M. Urbaniak, R. Goluch-Goreczna, A.K. Bledzki, Natural cork agglomerate as an ecological alternative in constructional sandwich composites, BioResources 12 (2017) http://dx.doi.org/10.15376/biores.12.3.5512-5524.

[16] J. Summerscales, J. Graham-Jones, R. Pemberton (Eds.), Marine Composites: Design and Performance, Woodhead, Duxford, UK, 2019.

[17] H. du Plessis, Fibreglass Boats, third ed., n.d.

[18] Eric Greene Associates, ed., Marine Composites, second ed., Eric Greene Associates, Annapolis, Md, 1999.

[19] R. Ferreira, D. Pereira, A. Gago, J. Proença, Experimental characterisation of cork agglomerate core sandwich panels for wall assemblies in buildings, J. Build. Eng. 5 (2016) 194–210, http://dx.doi.org/10.1016/j.jobe.2016.01.003.

[20] M.M. Mateus, J.M. Bordado, R.G. dos Santos, Ultimate use of Cork – Unorthodox and innovative applications, Ciênc. Tecnol. Mater. 29 (2017) 65–72, http://dx.doi.org/10.1016/j.ctmat.2016.03.005.

[21] R.M. Novais, L. Senff, J. Carvalheiras, M.P. Seabra, R.C. Pullar, J.A. Labrincha, Sustainable and efficient cork - inorganic polymer composites: An innovative and eco-friendly approach to produce ultra-lightweight and low thermal conductivity materials, Cem. Concr. Compos. 97 (2019) 107–117, http://dx.doi.org/10.1016/j.cemconcomp.2018.12.024.

[22] M. Najafi, A. Darvizeh, R. Ansari, Characterization of moisture effects on novel agglomerated cork core sandwich composites with fiber metal laminate facesheets, J. Sandw. Struct. Mater. 22 (2020) 1709–1742, http://dx.doi.org/10.1177/1099636218789613.

[23] C. Ihamouchen, H. Djidjelli, A. Boukerrou, Development and characterization of a new cork-based material, Mater. Today Proc. 36 (2021) 34–40, http://dx.doi.org/10.1016/j.matpr.2020.05.092.

[24] S. Gürgen, M.A. Sofuoğlu, Smart polymer integrated cork composites for enhanced vibration damping properties, Compos. Struct. 258 (2021) 113200, http://dx.doi.org/10.1016/j.compstruct.2020.113200.

[25] E.M. Fernandes, V.M. Correlo, J.F. Mano, R.L. Reis, Novel cork–polymer composites reinforced with short natural coconut fibres: Effect of fibre loading and coupling agent addition, Compos. Sci. Technol. 78 (2013) 56–62, http://dx.doi.org/10.1016/j.compscitech.2013.01.021.

[26] R. Hoto, G. Furundarena, J.P. Torres, E. Muñoz, J. Andrés, J.A. García, Flexural behavior and water absorption of asymmetrical sandwich composites from natural fibers and cork agglomerate core, Mater. Lett. 127 (2014) 48–52, http://dx.doi.org/10.1016/j.matlet.2014.04.088.

[27] P.T. Santos, S. Pinto, P.A.A.P. Marques, A.B. Pereira, R.J. Alves de Sousa, Agglomerated cork: A way to tailor its mechanical properties, Compos. Struct. 178 (2017) 277–287, http://dx.doi.org/10.1016/j.compstruct.2017.07.035.

[28] B. Soares, Sandwich Structures with Cork Based Cores (MSc), Instituto Superior Técnico, 2007.

[29] N. Pinto, A. Silva, L. Reis, Investigation of applicability of cork agglomerates in applications under shear strength, in: Proc. 8th Int. Conf. Sandw. Struct. ICSS 8, Porto, Portugal, 2008.
[30] L. Reis, A. Silva, Mechanical behavior of sandwich structures using natural cork agglomerates as core materials, J. Sandw. Struct. Mater. 11 (2009) 487–500, http://dx.doi.org/10.1177/1099636209104523.
[31] O. Castro, J.M. Silva, T. Devezas, A. Silva, L. Gil, Cork agglomerates as an ideal core material in lightweight structures, Mater. Des. 31 (2010) 425–432, http://dx.doi.org/10.1016/j.matdes.2009.05.039.
[32] S. Kim, D.R. Wallace, Flexural property of cork composite in a sandwich panel, in: ICSS-9 Book Abstr., California Institute of Technology Pasadena, California 91125, USA, 2010.
[33] J.M. Silva, T.C. Devezas, A. Silva, L. Gil, C. Nunes, N. Franco, Exploring the use of cork based composites for aerospace applications, Mater. Sci. Forum 636–637 (2010) 260–265, http://dx.doi.org/10.4028/www.scientific.net/MSF.636-637.260.
[34] M. Dumont, Application of Novel Cork Sandwich Core for High Performance Sailing Craft (MSc), University of Southampton, 2012.
[35] F. Balikoğlu, T.K. DemiRciOğlu, N. Arslan, The low-velocity impact behaviour of wood skinned sandwich composites with different core configurations, in: Proc. Int. For. Prod. Congr. Trabzon, Turkey, 2018, p. 13.
[36] T.K. Demircioğlu, F. Balıkoğlu, O. İnal, N. Arslan, İ. Ay, A. Ataş, Experimental investigation on low-velocity impact response of wood skinned sandwich composites with different core configurations, Mater. Today Commun. 17 (2018) 31–39, http://dx.doi.org/10.1016/j.mtcomm.2018.08.003.
[37] Y. Miyamoto, W.A. Kaysser, B.H. Rabin, A. Kawasaki, R.G. Ford (Eds.), Functionally Graded Materials, Springer US, Boston, MA, 1999, http://dx.doi.org/10.1007/978-1-4615-5301-4.
[38] L. Cui, S. Kiernan, M.D. Gilchrist, Designing the energy absorption capacity of functionally graded foam materials, Mater. Sci. Eng. A 507 (2009) 215–225, http://dx.doi.org/10.1016/j.msea.2008.12.011.
[39] E. Etemadi, A. Afaghi Khatibi, M. Takaffoli, 3D finite element simulation of sandwich panels with a functionally graded core subjected to low velocity impact, Compos. Struct. 89 (2009) 28–34, http://dx.doi.org/10.1016/j.compstruct.2008.06.013.
[40] A.F. Ávila, Failure mode investigation of sandwich beams with functionally graded core, Compos. Struct. 81 (2007) 323–330, http://dx.doi.org/10.1016/j.compstruct.2006.08.030.
[41] N. Gardner, E. Wang, A. Shukla, Performance of functionally graded sandwich composite beams under shock wave loading, Compos. Struct. 94 (2012) 1755–1770, http://dx.doi.org/10.1016/j.compstruct.2011.12.006.
[42] J. Zhou, Z.W. Guan, W.J. Cantwell, The impact response of graded foam sandwich structures, Compos. Struct. 97 (2013) 370–377, http://dx.doi.org/10.1016/j.compstruct.2012.10.037.
[43] B.O. Baba, Curved sandwich composites with layer-wise graded cores under impact loads, Compos. Struct. 159 (2017) 1–11, http://dx.doi.org/10.1016/j.compstruct.2016.09.054.
[44] C. Kaboglu, L. Yu, I. Mohagheghian, B.R.K. Blackman, A.J. Kinloch, J.P. Dear, Effects of the core density on the quasi-static flexural and ballistic performance of fibre-composite skin/foam-core sandwich structures, J. Mater. Sci. 53 (2018) 16393–16414, http://dx.doi.org/10.1007/s10853-018-2799-x.
[45] S. Petit, C. Bouvet, A. Bergerot, J.-J. Barrau, Impact and compression after impact experimental study of a composite laminate with a cork thermal shield, Compos. Sci. Technol. 67 (2007) 3286–3299, http://dx.doi.org/10.1016/j.compscitech.2007.03.032.
[46] A.T. Nettles, J.R. Jackson, A.J. Hodge, Change in damage tolerance characteristics of sandwich structure with a thermal protection system (TPS), J. Compos. Mater. 46 (2012) 211–226, http://dx.doi.org/10.1177/0021998311410509.
[47] J. Sargianis, H. Kim, J. Suhr, Natural cork agglomerate employed as an environmentally friendly solution for quiet sandwich composites, Sci. Rep. 2 (2012) 403, http://dx.doi.org/10.1038/srep00403.
[48] B. Hachemane, R. Zitoune, B. Bezzazi, C. Bouvet, Sandwich composites impact and indentation behaviour study, Composites B 51 (2013) 1–10, http://dx.doi.org/10.1016/j.compositesb.2013.02.014.
[49] R. Fernandes, M.F.S.F. de Moura, F.G.A. Silva, N. Dourado, Mode I fracture characterization of a hybrid cork and carbon–epoxy laminate, Compos. Struct. 112 (2014) 248–253, http://dx.doi.org/10.1016/j.compstruct.2014.02.019.
[50] M.F.S.F. de Moura, R. Fernandes, F.G.A. Silva, N. Dourado, Mode II fracture characterization of a hybrid cork/carbon-epoxy laminate, Composites B 76 (2015) 44–51, http://dx.doi.org/10.1016/j.compositesb.2015.02.010.
[51] M.R. Sheikhi, S. Gürgen, Anti-impact design of multi-layer composites enhanced by shear thickening fluid, Compos. Struct. 279 (2022) 114797, http://dx.doi.org/10.1016/j.compstruct.2021.114797.
[52] R. Selvaraj, A. Maneengam, M. Sathiyamoorthy, Characterization of mechanical and dynamic properties of natural fiber reinforced laminated composite multiple-core sandwich plates, Compos. Struct. 284 (2022) 115141, http://dx.doi.org/10.1016/j.compstruct.2021.115141.
[53] A. Gomez, E. Barbero, S. Sanchez-Saez, Modelling of carbon/epoxy sandwich panels with agglomerated cork core subjected to impact loads, Int. J. Impact Eng. 159 (2022) 104047, http://dx.doi.org/10.1016/j.ijimpeng.2021.104047.
[54] Q. Ma, M. Rejab, J. Siregar, Z. Guan, A review of the recent trends on core structures and impact response of sandwich panels, J. Compos. Mater. 55 (2021) 2513–2555, http://dx.doi.org/10.1177/0021998321990734.
[55] P.N.B. Reis, M.P. Silva, P. Santos, J.M. Parente, S. Valvez, A. Bezazi, Mechanical performance of an optimized cork agglomerate core-glass fibre sandwich panel, Compos. Struct. 245 (2020) 112375, http://dx.doi.org/10.1016/j.compstruct.2020.112375.
[56] S. Prabhakaran, V. Krishnaraj, K. Shankar, M. Senthilkumar, R. Zitoune, Experimental investigation on impact, sound, and vibration response of natural-based composite sandwich made of flax and agglomerated cork, J. Compos. Mater. 54 (2020) 669–680, http://dx.doi.org/10.1177/0021998319871354.
[57] M. Najafi, A. Darvizeh, R. Ansari, Characterization of moisture effects on novel agglomerated cork core sandwich composites with fiber metal laminate facesheets, J. Sandw. Struct. Mater. 22 (2020) 1709–1742, http://dx.doi.org/10.1177/1099636218789613.
[58] I. Ivañez, S. Sánchez-Saez, S.K. Garcia-Castillo, E. Barbero, A. Amaro, P.N.B. Reis, High-velocity impact behaviour of damaged sandwich plates with agglomerated cork core, Compos. Struct. 248 (2020) 112520, http://dx.doi.org/10.1016/j.compstruct.2020.112520.
[59] F. Sarasini, J. Tirillò, L. Lampani, M. Sasso, E. Mancini, C. Burgstaller, A. Calzolari, Static and dynamic characterization of agglomerated cork and related sandwich structures, Compos. Struct. 212 (2019) 439–451, http://dx.doi.org/10.1016/j.compstruct.2019.01.054.
[60] P. Kaczynski, M. Ptak, J. Wilhelm, F.A.O. Fernandes, R.J.A. de Sousa, High-energy impact testing of agglomerated cork at extremely low and high temperatures, Int. J. Impact Eng. 126 (2019) 109–116, http://dx.doi.org/10.1016/j.ijimpeng.2018.12.001.
[61] G. Sun, E. Wang, H. Wang, Z. Xiao, Q. Li, Low-velocity impact behaviour of sandwich panels with homogeneous and stepwise graded foam cores, Mater. Des. 160 (2018) 1117–1136, http://dx.doi.org/10.1016/j.matdes.2018.10.047.
[62] P. Sadeghian, D. Hristozov, L. Wroblewski, Experimental and analytical behavior of sandwich composite beams: Comparison of natural and synthetic materials, J. Sandw. Struct. Mater. 20 (2018) 287–307, http://dx.doi.org/10.1177/1099636216649891.
[63] T.K. Demircioğlu, F. Balıkoğlu, O. İnal, N. Arslan, İ. Ay, A. Ataş, Experimental investigation on low-velocity impact response of wood skinned sandwich composites with different core configurations, Mater. Today Commun. 17 (2018) 31–39, http://dx.doi.org/10.1016/j.mtcomm.2018.08.003.
[64] F. Balıkoğlu, T.K. Demircioğlu, O. İnal, N. Arslan, A. Ataş, Compression after low velocity impact tests of marine sandwich composites: Effect of intermediate wooden layers, Compos. Struct. 183 (2018) 636–642, http://dx.doi.org/10.1016/j.compstruct.2017.08.003.
[65] M. Ptak, P. Kaczynski, F.A.O. Fernandes, R.J.A. de Sousa, Assessing impact velocity and temperature effects on crashworthiness properties of cork material, Int. J. Impact Eng. 106 (2017) 238–248, http://dx.doi.org/10.1016/j.ijimpeng.2017.04.014.
[66] M.F.S.F. de Moura, P.M.L.C. Cavaleiro, F.G.A. Silva, N. Dourado, Mixed-mode I+II fracture characterization of a hybrid carbon-epoxy/cork laminate using the Single-Leg Bending test, Compos. Sci. Technol. 141 (2017) 24–31, http://dx.doi.org/10.1016/j.compscitech.2017.01.001.
[67] H. Wang, K.R. Ramakrishnan, K. Shankar, Experimental study of the medium velocity impact response of sandwich panels with different cores, Mater. Des. 99 (2016) 68–82, http://dx.doi.org/10.1016/j.matdes.2016.03.048.
[68] F.C. Potes, J.M. Silva, P.V. Gamboa, Development and characterization of a natural lightweight composite solution for aircraft structural applications, Compos. Struct. 136 (2016) 430–440, http://dx.doi.org/10.1016/j.compstruct.2015.10.034.
[69] N. Lakreb, B. Bezzazi, H. Pereira, Mechanical behavior of multilayered sandwich panels of wood veneer and a core of cork agglomerates, Mater. Des. 1980-2015 65 (2015) 627–636, http://dx.doi.org/10.1016/j.matdes.2014.09.059.
[70] A. Lagorce-Tachon, T. Karbowiak, D. Champion, R.D. Gougeon, J.-P. Bellat, Mechanical properties of cork: Effect of hydration, Mater. Des. 82 (2015) 148–154, http://dx.doi.org/10.1016/j.matdes.2015.05.034.
[71] F.A.O. Fernandes, R.T. Jardin, A.B. Pereira, R.J. Alves de Sousa, Comparing the mechanical performance of synthetic and natural cellular materials, Mater. Des. 82 (2015) 335–341, http://dx.doi.org/10.1016/j.matdes.2015.06.004.
[72] Amorim Cork Composites, Corecork NL20 Material Datasheet, Amorim Cork Composites, 2017.
[73] D.A. Winter, Biomechanics and Motor Control of Human Gait, second ed., Univ. of Waterloo Press, Waterloo, Ontario, 1991.
[74] L.S. Sutherland, M.F. Sá, J.R. Correia, C. Guedes Soares, A. Gomes, N. Silvestre, Quasi-static indentation response of pedestrian bridge multicellular pultruded GFRP deck panels, Constr. Build. Mater. 118 (2016) 307–318, http://dx.doi.org/10.1016/j.conbuildmat.2016.05.070.
[75] L.S. Sutherland, C. Guedes Soares, The use of quasi-static testing to obtain the low-velocity impact damage resistance of marine GRP laminates, Composites B 43 (2012) 1459–1467, http://dx.doi.org/10.1016/j.compositesb.2012.01.002.
[76] L.S. Sutherland, M.F. Sá, J.R. Correia, C. Guedes Soares, A. Gomes, N. Silvestre, Impact response of pedestrian bridge multicellular pultruded GFRP deck panels,

Compos. Struct. 171 (2017) 473–485, http://dx.doi.org/10.1016/j.compstruct.2017.03.052.
[77] ASTM, ASTM D7766-11 Standard Practice for Damage Resistance Testing of Sandwich Constructions, ASTM International, 2011.
[78] ASTM, ASTM D6264-12 Standard Test Method for Measuring the Damage Resistance of a Fiber-Reinforced Polymer-Matrix Composite to a Concentrated Quasi-Static Indentation Force, ASTM International, 2012.
[79] ASTM, ASTM D7136-15 Standard Test Method for Measuring the Damage Resistance of a Fiber-Reinforced Polymer Matrix Composite to a Drop-Weight Impact Event, ASTM International, 2015.
[80] L.S. Sutherland, C. Guedes Soares, Impact tests on woven-roving E-glass/polyester laminates, Compos. Sci. Technol. 59 (1999) 1553–1567, http://dx.doi.org/10.1016/S0266-3538(99)00023-8.
[81] M. Garrido, R. Teixeira, J. Correia, L.S. Sutherland, Quasi-static indentation and impact in glass-fibre reinforced polymer sandwich panels for civil and ocean engineering applications, J. Sandw. Struct. Mater. (2019) 109963621983013, http://dx.doi.org/10.1177/1099636219830134.
[82] ASTM, ASTM C393-11 Standard Test Method for Core Shear Properties of Sandwich Constructions by Beam Flexure, ASTM International, 2011.
[83] ASTM, ASTM C393-00 Standard Test Method for Flexural Properties of Sandwich Constructions, ASTM International, 2000.
[84] E.A. Kotsidis, I.G. Kouloukouras, N.G. Tsouvalis, Composite Materials Manufacturing and Characterization (Deliverable D2.2), NTUA, 2013.
[85] ASTM, ASTM D7249-12 Standard Test Method for Facing Properties of Sandwich Constructions by Long Beam Flexure, 2012.
[86] 3A Core Materials, AIREX C70 Datasheet, 3A Core Materials, 2011.